

# AN INTEGRATED MULTI-CHANNEL SYSTEM FOR BIOMEDICAL SIGNAL ACQUISITION

Jakob M. Tomasik, Wjatscheslaw Galjan, Kristian M. Hafkemeyer  
Dietmar Schroeder and Wolfgang H. Krautschneider  
*Institute of Nanoelectronics, Hamburg University of Technology, Eissendorfer Str. 38  
D-21073 Hamburg, Hamburg, Germany*

**Keywords:** Biomedical signals, SoC, Low-power, Low-noise, Configurable, CMRR-calibration, DC-suppression.

**Abstract:** A CMOS configurable system-on-chip (SoC) for biomedical signal acquisition is described. The SoC is composed of 10 channels, each channel including a programmable analog front-end (AFE) and a 20 bit analog-to-digital converter (ADC). The digitized signals are read out via a high-speed serial communication bus. The AFE includes a common-mode rejection ratio (CMRR) calibration circuitry resulting in a CMRR of more than 80 dB and an active DC-suppression circuitry giving the DC-coupled instrumentation amplifier the possibility to tolerate DC-offsets of up to  $\pm 1$  V for a power supply voltage of 3.3 V. In low-noise mode the AFE achieves an input referred noise of less than 50 nVrms for EEG application (0.5-70 Hz) and the power consumption of a channel including AFE and ADC is less than 5 mW in low-power mode. A prototype has been fabricated in a 0.35  $\mu$ m CMOS process.

## 1 INTRODUCTION

The integration of biomedical signal acquisition systems in CMOS technology allows not only a reduction of costs for traditional medical devices, but also facilitates portable long-term applications or implantable solutions. As part of an integrated solution, designs of a complete analog front-end (AFE) have been reported (Martins et al., 1998; Ng and Chan, 2005; Yazicioglu, 2007). In addition, Desel et al. (1996) and Fuchs et al. (2002) describe system-on-chip (SoC) implementations including also analog-to-digital conversion (ADC) and digital IO interfacing.

To cover the wide range of biomedical signals the system should be adaptable to their characteristics. The flexibility of a system means to provide an optimal setting of the overall system with respect to the signal type and system application. In this context, the AFE is the prime candidate for configurability. Two complementary application examples illustrate this: For portable long-term monitoring of electrocardiogram (ECG) signals the system's power consumption plays an essential role whereas noise constraints are rather relaxed (Martin et al., 2000; Galjan et al., 2008). In contrast to this, for extremely sensitive evoked potential (EP)

recordings (Scheer et al., 2006), low-noise amplification of the signal is crucial at the expense of rather high power consumption. Including these two extreme settings, a configurable biomedical signal acquisition system should be adaptable to a variety of signal types. Table 1 shows the associated signal characteristics based on (Bronzino, 2000; Webster, 1998).

Table 1: Characteristics of biomedical signals.

Signal Type*	Signal Bandwidth	Signal Amplitude
ECG	0.05 Hz–250 Hz	5 $\mu$ Vpp – 8 mVpp
EEG	0.05 Hz – 70 Hz	2 $\mu$ Vpp – 200 $\mu$ Vpp
EMG	0.01 Hz – 5 kHz	50 $\mu$ Vpp – 10 mVpp
EP	0.1 Hz – 3 kHz	20 nVpp – 20 $\mu$ Vpp

\*ECG: electrocardiogram, EEG: electroencephalogram, EMG: electromyogram, EP: evoked potentials.

Two additional requirements are inherently typical for biomedical signal acquisition systems: A high common-mode rejection ratio (CMRR) (in particular at 50/60 Hz) and large electrode DC-offset handling capability. The need for a high CMRR results from power line interferences inducing a common mode voltage present at the amplifier's

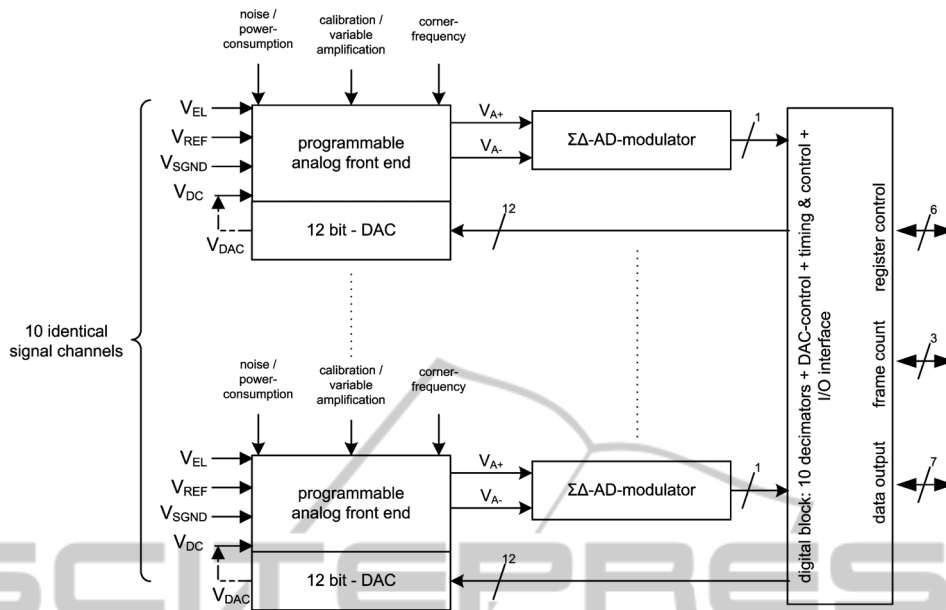


Figure 1: Block diagram of the system-on-chip.

input (Webster, 1998). Large DC-offsets (i.e. hundreds of millivolts) may arise from the electrode-skin interface (Webster, 1998) and require counter measures to prevent saturation of the instrumentation amplifier (IA). Finally, a biomedical SoC should provide a digital interface for simple configuration of the system and a high speed data output for read out of the acquired biomedical signals.

In this work we present a configurable SoC for biomedical signal acquisition including CMRR-calibration and DC-offset suppression. A first approach for the SoC has been described in (Van Helleputte et al., 2008) and first simulation results of this system have been presented in (Hafkemeyer et al., 2007). This paper is organized as follows: Section 2 gives an overview of the system. In Section 3 we describe the analog front-end, in Section 4 the analog-to-digital converter is presented, and in Section 5 the digital IO interface is described. In Section 6 we present the measurement results and discussion and conclusion are finally contained in Section 7.

## 2 SYSTEM OVERVIEW

The block diagram of the SoC is presented in Figure 1. The main components of this SoC are 10 identical channels and a digital block. Each channel includes an AFE, a  $\Sigma\Delta$ -modulator and a 12-bit digital-to-analog converter (DAC) for DC-offset

suppression of the associated channel. The AFE's inputs are the electrode input ( $V_{EL}$ ), the reference signal ( $V_{REF}$ ), signal ground ( $V_{SGND}$ ) and DC-suppression voltage ( $V_{DC}$ ). Whereas  $V_{EL}$ ,  $V_{REF}$  and  $V_{SGND}$  are familiar IA inputs, the  $V_{DC}$  input is used to suppress the input DC-offset voltage and is driven by the DAC output ( $V_{DAC}$ ).

Subsequent to the AFE the  $\Sigma\Delta$ -modulator generates a 1-bit stream which is decimated to perform the analog-to-digital conversion. The digital block contains 10 decimation filters for this purpose. Additional functions of the digital block include the control of the DAC, timing and SoC's sub blocks. Finally, the digital block enables communication to and from the chip. This comprises setting the internal registers (register control), reading out the measured data (data output) and synchronizing the measured data if several chips are used on the same bus (frame count).

## 3 ANALOG FRONT-END

A block diagram of the programmable analog front-end is given in Figure 2a. The IA amplifies the applied signal with a constant factor of 4. The signal is fed into the postamplifier directly or via an external high-pass filter.

The postamplifier's gain is configurable with amplification factors of 5, 20, 40 and 80 resulting in the desired channel gain factors of 20, 80, 160 and 320. Following the postamp a low-pass filter acts as

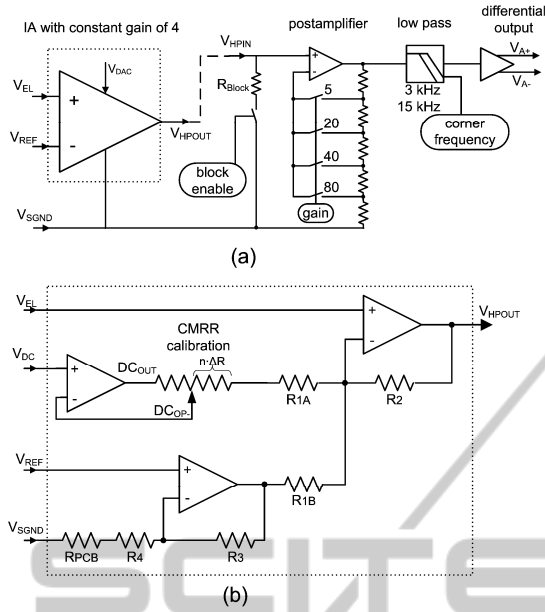


Figure 2: (a) Structure of the programmable analog front-end, (b) detailed view of the IA.

an anti-aliasing filter for the ADC. The low-pass corner frequency can be set to be either 3 kHz (ECG, EEG) or 15 kHz (EMG, EP). Finally, the single-ended signal is converted to a differential one as required by the subsequent  $\Sigma\Delta$ -modulator. The design specifications for the AFE are given in Table 2.

### 3.1 Instrumentation Amplifier with CMRR-calibration

The IA used as a preamplifier in the AFE is implemented by using a modified 2-opamp IA architecture and is presented in Figure 2b. The modification is composed of a third opamp for subtracting any DC-offset using the DAC generated voltage  $V_{DC}$ . The additional circuitry also incorporates a digitally controlled tunable resistor for CMRR-calibration, the resistor's step size is denoted as  $\Delta R$ . For modeling parasitic PCB or bond wire resistances at the signal ground input  $V_{SGND}$  a resistor  $R_{PCB}$  has been added in Fig 2b. The IA's transfer function with respect to  $V_{SGND}$  is given by:

$$V_{HPOUT} = V_{EL} \left( 1 + \frac{R_2}{R_{1A^*}} + \frac{R_2}{R_{1B}} \right) - V_{REF} \frac{R_2}{R_{1B}} \left( 1 + \frac{R_3}{R_{4^*}} \right) - V_{DC} \frac{R_2}{R_{1A^*}}, \quad (1)$$

with  $R_{1A^*} = R_{1A} + n \cdot \Delta R$  and  $R_{4^*} = R_4 + R_{PCB}$ .

A differential gain  $G$  between  $V_{EL}$  and  $V_{REF}$  is obtained from (1) by setting the values for  $R_1$ ,  $R_2$ ,  $R_3$

Table 2: Design specifications for the analog front-end.

Parameter	Conditions/Remarks	Value
Signal input range	Ext. programmable	$\pm 5$ mV $\pm 20$ mV $\pm 40$ mV $\pm 80$ mV
Offset comp. range	0.01 Hz – 5 kHz	$\pm 1000$ mV @ $V_{DD} = 3.3$ V
Total input referred noise	0.05 Hz – 250 Hz (ECG) 0.05 Hz – 70 Hz (EEG) 0.01 Hz – 5 kHz (EMG) 0.1 Hz – 3 kHz (EP)	$< 4.7$ $\mu$ Vpp $< 1.0$ $\mu$ Vpp $< 6.0$ $\mu$ Vpp $< 2.2$ $\mu$ Vpp
CMRR	@ 50 Hz	$> 80$ dB

and  $R_4$  (neglecting  $R_{PCB}$  and assuming  $R_1 = R_{1A^*} = R_{1B}$  and  $V_{DC} = 0$  V) such that the terms in front of  $V_{EL}$  and  $V_{REF}$  have both the same value  $G$ . In this case the gain  $G$  is equal to

$$G = \frac{V_{HPOUT}}{V_{EL} - V_{REF}} = 2 \frac{R_2}{R_1} + \frac{R_3}{R_4} - \frac{R_1}{R_2}. \quad (2)$$

In the presented circuit a gain value of  $G = 4$  has been obtained by using resistor values of  $R_1 = 1$  k $\Omega$ ,  $R_2 = 1.5$  k $\Omega$ ,  $R_3 = 1$  k $\Omega$  and  $R_4 = 600$   $\Omega$ .

If any DC-offset is present at the input, the aforementioned voltage  $V_{DC}$  scaled by a factor  $R_2/R_{1A}$  is subtracted from the IA's output voltage  $V_{HPOUT}$ . The result of this action is a cancellation of DC-offsets up to a value of

$$V_{EL,dcmax} = \frac{V_{DD}}{2G} \frac{R_2}{R_1}. \quad (3)$$

Using above values for  $R_1$ ,  $R_2$  and  $G$  and a power supply voltage  $V_{DD}$  of 3.3 V, a maximal DC-offset of  $V_{EL,dcmax} = \pm 619$  mV is obtained. In conjunction with the external high pass filter and a postamplifier gain of 80 the specified offset compensation range of  $\pm 1000$  mV is reached.

The CMRR calibration compensates for any mismatch in the resistors  $R_1$  to  $R_4$  and wiring parasitics  $R_{PCB}$ . The calibration circuit has been located in the high-resistive feedback loop of the DC-offset compensation opamp to minimize non-idealities. By changing the tap-point in the feedback path of the DC-offset compensation opamp a value of  $n\Delta R$  is added to the resistor  $R_{1A}$ . The CMRR of the IA becomes

$$CMRR = \frac{1 + \frac{R_2}{R_{1A} \pm n\Delta R} + \frac{R_2}{R_{1B}}}{1 + \frac{R_2}{R_{1A} \pm n\Delta R} \left( 1 + \frac{R_3}{R_4} \right)}. \quad (4)$$

It should be taken into account that a variation of  $R_{1A}$  also affects the differential gain  $G$ . Therefore resistor values should be chosen such that the gain error between channels does not exceed 1%. A CMRR value of more than 80 dB (including  $R_{PCB}$ ) is achieved by using a step size  $\Delta R < 0.26 \Omega$  and  $n = 64$  steps. Using a driven right leg system (Winter, 1983) for patient grounding the overall CMRR is increased by approx. 40 dB resulting in a system CMRR of 120 dB.

The configurability of the IA regarding noise/power- consumption is realized using the programmable operational amplifier described in (Bronskowski and Schroeder, 2006). These opamps use chopper modulation to reduce  $1/f$ -noise and can be programmed in a wide range between ultra low-noise ( $2 \text{ nV}/\sqrt{\text{Hz}}$ ) and low-power consumption ( $140 \mu\text{W}$ ).

### 3.2 Postamplifier and External Highpass Filter

The postamplifier is composed of the same programmable opamp as the IA. It is used in a non-inverting configuration having four gain settings (5, 20, 40 and 80). These are realized by a resistor chain having four taps. Connecting one of the taps to the opamp's inverting input using a CMOS switch sets the appropriate gain factor. Care has to be taken regarding the accuracy of the resistors to fulfill the specified gain error between channels ( $<1\%$ ). Chopper modulation of the opamp is also needed in the postamplifier due to the low preamplifiers' gain factor of 4 for low-noise applications.

The optional external passive high pass filter can be placed between the  $V_{HPOUT}$  output pin of the IA and the postamplifier's input pin  $V_{HPIN}$  (dashed line in Figure 2a). Using external components for the high pass filter (i.e. capacitor and resistor) eases the implementation of the large time constants needed.

A drawback of the large time constant arises if events like external stimulation or movements of the electrodes induce a noticeable shift in the DC-potential of the external capacitor: the time for restoring the system back to equilibrium is determined by the time constant of the high pass filter, i.e. in range of seconds. To overcome this problem an additional switch has been placed to discharge the capacitor over the relative small resistor  $R_{Block}$ . The signal to close the switch ("block enable" in Figure 2a) can be set via the serial configuration port.

### 3.3 Low-pass Filter and Symmetry Stage

The  $\Sigma\Delta$ -analog-to-digital conversion requires an anti-aliasing filter preceding the  $\Sigma\Delta$ -modulator. In contrast to Nyquist-rate ADCs the anti-aliasing filter's cut-off frequencies are rather easy to implement with oversampling ADCs, where the relative low bandwidths of the biomedical signals would lead to large time constants and hence require external components. The anti-aliasing filter is implemented as a second-order low-pass filter using an opamp in a Sallen&Key configuration (Allen and Holberg, 2002). To choose the cut-off frequency, the maximum signal frequency, the oversampling ratio and the needed signal attenuation have to be considered. Choosing an attenuation of more than 40 dB at half of the oversampling frequency and an oversampling ratio of 256, cut-off frequencies of 3 kHz for ECG/EEG and 15 kHz for EMG/EP ensure proper anti-aliasing functionality. The cut-off frequency can be configured externally via the serial configuration port.

Following the low-pass filter a symmetry stage converts the single-ended signal ( $V_{A+}$ ) into a differential one using an opamp to obtain the inverted signal ( $V_{A-}$ ). These signals are fed into the succeeding  $\Sigma\Delta$ -modulator. Additional care has to be taken to keep these signals stable at the modulators input because of its switching operation (Maxim Integrated Products, 2000). Therefore, an integrated low-path RC-filter with  $R = 5 \text{ k}\Omega$  and  $C = 2.5 \text{ pF}$  has been inserted between the symmetry stage outputs and the  $\Sigma\Delta$ -modulator inputs.

## 4 ADC

Analog-to-digital conversion for each channel is accomplished by a 2<sup>nd</sup>-order  $\Sigma\Delta$ -modulator and a decimation filter. The default oversampling ratio (OSR) of the  $\Sigma\Delta$ -modulator is 256, the OSR can be changed using the serial configuration port to a value of  $\text{OSR} = 256 \pm 128$  (in steps of 1). The sampling rate at the modulator's input is derived from the 12.8 MHz main clock using on-chip division by  $(n + 1)$ . Like the OSR,  $n$  can be set by programming and has a value range from  $n = 0$  to  $n = 255$ . For example, using an oversampling ratio of 256 and setting  $n$  to 0 or 249 data rates (DR) of 50 kHz and 200 Hz can be achieved, respectively.

## 4.1 Sigma-Delta Modulator

The 2<sup>nd</sup>-order  $\Sigma\Delta$ -modulator is implemented as a discrete time 1-bit modulator. The circuit topology of the switched-capacitor  $\Sigma\Delta$ -modulator is derived from (Medeiro et al., 1997) and a modified version also used in the present topology has already been used in (Fuchs et al., 2002). The sizing of the actual capacitors used for the switched capacitor integrators results in signal-transfer and noise-transfer functions (STF and NTF) (Fuchs, 2004):

$$STF(z) = \frac{1}{8z^2 - 14z + 7} \quad (5)$$

and

$$NTF(z) = \frac{8z^2 - 16z + 8}{8z^2 - 14z + 7}. \quad (6)$$

The required effective number of bits (ENOB) of the  $\Sigma\Delta$ -modulator is depending on the signal type: For EEG approx. 16 bits or a dynamic range (DR) of 98 dB are required whereas for ECG 12 bits or a dynamic range of 74 dB is sufficient.

## 4.2 Decimation Filter

Decimation and low-pass filtering of the modulator's output signal is accomplished using a comb filter having a  $\text{sinc}^3(f)$  frequency response. The implemented filter uses decomposition and modulo arithmetic to minimize the system size (Dijkstra et al., 1988). The decimation filters block diagram is shown in Figure 3. The input signal  $x(n)$  at oversampling frequency is first integrated by a 3<sup>rd</sup> order IIR filter. Next, decimation by a factor  $M$  is carried out to obtain the final data rate. Finally, a 3<sup>rd</sup> order FIR differentiator generates the output of the decimation filter.

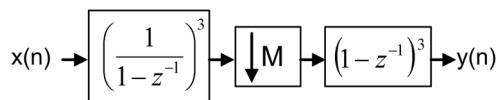


Figure 3: Block diagram of the decimator.

## 5 DIGITAL SYSTEM CONTROL AND INTERFACE

The communication to external components like a DSP or FPGA is realized by two independent serial ports. Therefore, the data and control paths are strongly separated. Figure 4 shows an overview of the signal and control flows. Serial configuration

port receives the control data and applies it to the sub-blocks even for the high speed dataport, setting up the data rate and the format of the transmission. For testing purposes of the digital data transmission the input of the decimator filters can be switched to the on-chip signal generators. These generators are based on the principle of digital resonators and are capable of generating precise sine waves (Lu and Roberts, 1994).

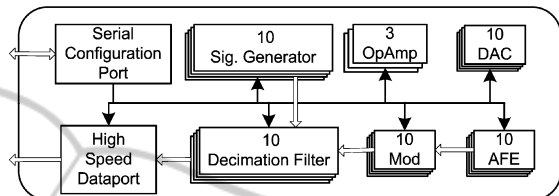


Figure 4: Digital system control and interface.

## 5.1 DC-suppression Feedback Circuit

Offset suppression of each electrode is realized by an additional input of the AFE. If this feature is not needed (e.g. for ECG application) this input can be connected to the virtual ground node. For applications with very small amplitudes (e.g. EEG) the electrode offset should be removed allowing the required high amplification factor of the data path. In this case, as shown in (1), the on-chip DACs are used to generate the subtracting voltage.

The input of the DACs can be switched between a value which is written into the configuration register by the serial control port or the output of the on-chip digital integrator. This integrator sums up the bit-stream generated by the modulator and is configurable by the serial configuration port for different time constants. To avoid noise of the high resistive output node (100 k $\Omega$ ) of the connected DAC and to smooth the nonlinearities caused by value changing of the DAC, a capacitor in the range between 1  $\mu\text{F}$  and 10  $\mu\text{F}$  should be added between the  $V_{\text{DAC}}$  output and signal ground.

For the implementation of the DAC a R-2R architecture (Allen and Holberg, 2002) was chosen and is depicted in Figure 5, where the inputs  $D_0$ - $D_{11}$  are connected to a 12-bit register. This DAC occupies an area of 0.5 mm<sup>2</sup> and consumes only 33  $\mu\text{A}$ .

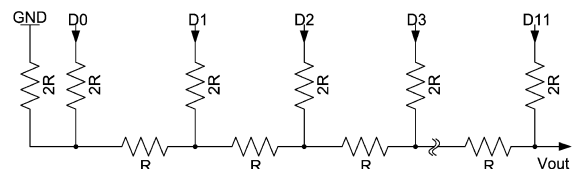


Figure 5: R-2R architecture of implemented 12-bit DAC.

### 5.2 Serial Configuration Port

The serial communication for setting up the system is realized by a synchronous bidirectional interface and is shown in Figure 6. The access to one of the hundred 8-bit registers is decoupled from other on-chip components and can be done asynchronously to the conversion clock and to the clock of the high speed serial dataport. Depending on the external interconnects the maximum bus speed can be used up to 100 kHz. This allows continuously to set up the DACs for offset cancellation and the external 16 General Purpose Outputs (GPOs) for controlling the possible external components during operation.

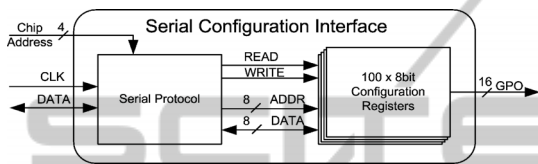


Figure 6: Block diagram of the serial configuration port.

### 5.3 High Speed Serial Dataport

The data from the SoC are read out by the high speed serial dataport which is synchronous to an applied clock signal, Figure 7 shows its block diagram. The receiver is synchronized to a new data packet by the framesync signal. The rising edge of this signal determines the new transmission, therefore, after a delay of one bit, the second bit is taken as valid data. Busrequest and bushold signals implement the handshake protocol allowing daisy chaining of 16 SoCs, this number is determined by the 4-bit chip address.

The serial data from one SoC includes a 22 x 16-bit wide packet which is sent for each sampled value of 10 channels. For a maximum data rate of 50k packets per second a minimum clock transmission frequency of  $352 \times 50k = 17.6$  MHz is needed. Hence, using the SoC in daisy chained application the maximum operating frequency of this high speed port is specified to 53 MHz to allow the data transmission of 3 SoCs.

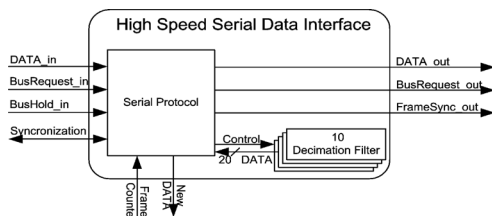


Figure 7: Block diagram of the high-speed serial dataport.

Table 3 shows the implemented protocol for one data packet. The 1st word contains the start marker FF9h and the chip address which is set by external digital 4-bit port. The 2nd transmitted word is the frame counter value. The 3rd word consists of the upper 16-bit data of the first channel. The 4th data word (bit 15..12) consists of the 4 lower data bits of the first channel (channel <0>) and the actual DAC value for the same channel. The following 18 words are in the same scheme as for the first channel (3rd and 4th words).

Table 3: Implemented protocol for the high speed data-port.

16 bit words	MSB		LSB	
	nibble		nibble	
	high	low	high	low
Word1	Fh	Fh	9h	chip address
Word2	framecounter			
Word3	upper 16 bits of ch. <0> data			
Word4	lower 4 bits of data	DAC value for ch. <0>		
Word5	upper 16 bits of ch. <1> data			
Word6	lower 4 bits of data	DAC value for ch. <1>		

## 6 RESULTS

A prototype of the SoC has been realized in a 0.35 μm CMOS process with a supply voltage of 3.3 V. To prevent coupling effects between digital and analog blocks, care has been taken to separate these parts in the layout. The power supply is likewise separated; additional on-chip stabilizing-capacitors are used for blocking off switching activities on the supply rails. These capacitors, which have been realized as poly-capacitors and Metal-Insulator-Metal (MIM) capacitors, also allow to fulfill the needed layer density specified by the foundry. Additional efforts have been taken to minimize resistive parasitics of the interconnects, this applies in particular to the supply rails and the connections to signal ground ( $V_{SGND}$ ).

A special approach was taken for the chopper clock lines: To minimize coupling effects to the analog parts due to high frequency switching operation each chopper clock path has been placed between two paths tied to ground.

A microphotograph of the fabricated SoC prototype is shown in Figure 8. The SoC occupies an area of 47 mm<sup>2</sup> and the number of pins is 144.

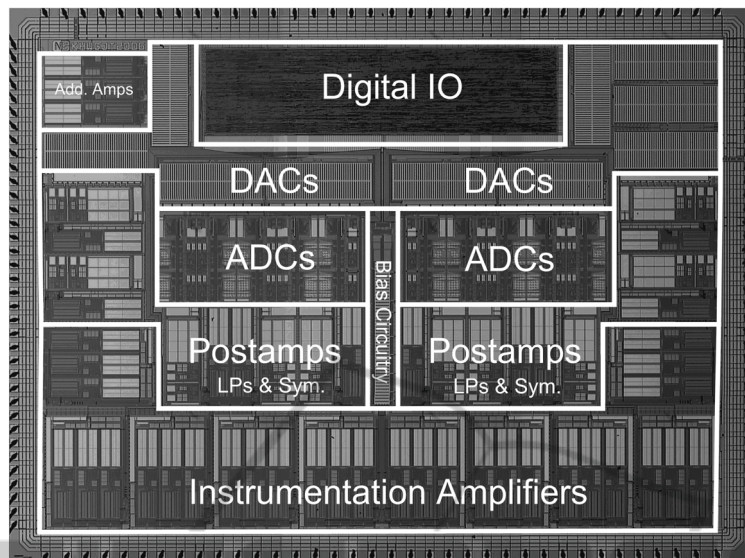


Figure 8: Microphotograph of the system-on-chip.

### 6.1 Analog Channel and CMRR Calibration

The measured overall gains (20, 80, 160 and 320) of analog channels for a bandwidth of 3 kHz are shown in Figure 9, therein the external high-pass filter is shorted and the DC-suppression is disabled. The input referred offset of the channels (with enabled chopper modulation) is less than 34  $\mu\text{V}$  and 12  $\mu\text{V}$  for the low-power and low-noise mode, respectively.

The DC-suppression circuit has been tested by applying a 500 mV<sub>pp</sub> square-wave to the input of the IA. This signal and the output of the IA are shown in Figure 10. The time constant of the on-chip digital integrator has been set to approximately one second. The IA saturates after the rising or falling edges of the square wave. Due to regulation of the activated DC-suppression, the offset voltage is subtracted from the channel resulting in an offset free output at signal ground ( $V_{\text{SGND}} = 1.65 \text{ V}$ ).

The CMRR calibration of all 10 channels is shown in Figure 11. The sweep of the implemented 64 calibration steps results in a channel CMRR of more than the specified 80 dB at 50 Hz for at least one calibration value.

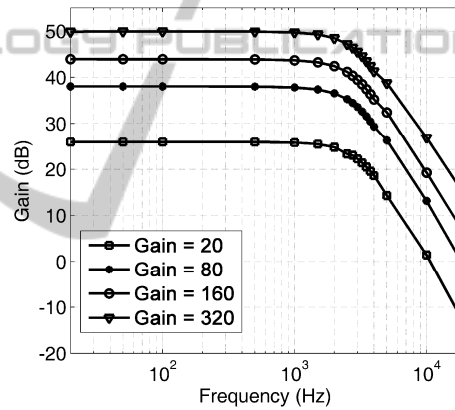


Figure 9: Measured gain and bandwidth of an analog channel. Markers indicate measured data points.

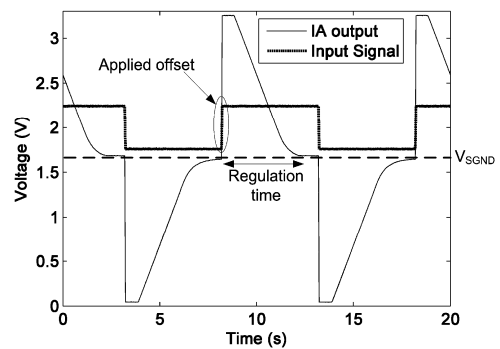


Figure 10: Example of the DC-suppression using a square-wave input, the IA output settles back to signal ground after the regulation time.

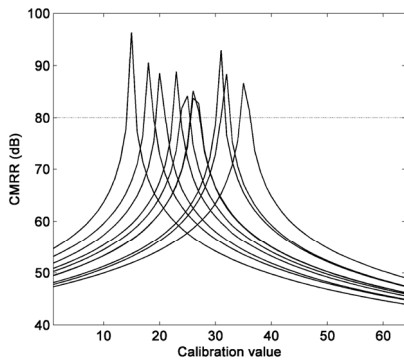


Figure 11: CMRR @ 50 Hz calibration of 10 channels.

### 6.2 Noise and Power

The total input referred noise has been measured including the full channel, i.e. the AFE,  $\Sigma\Delta$ -modulator and decimation filter. Figure 12 shows the influence of the chopper modulation for an ECG application and Table 4 summarizes the noise performance of the SoC.

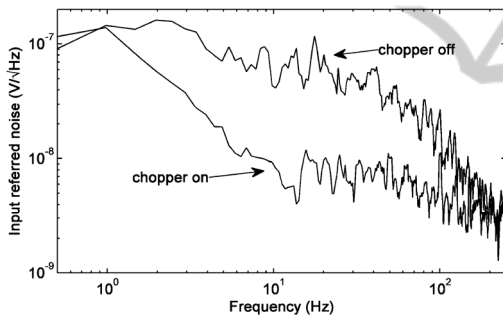


Figure 12: Input referred noise density for ECG bandwidth with chopper modulation on and off.

The power consumption of the SoC varies between 28.7 mW in low-power mode and 209.8 mW in low-noise mode for data rates of 500 Hz and 50 kHz, respectively.

Table 4: Measured total input referred noise at ADC output.

Integration Bandwidth (Signal Type)	Conditions/Remarks	Value $\mu\text{Vpp}$
0.05 Hz – 250 Hz (ECG)	Low-power, chopper enabled	1.13 – 1.74
	Low-power, chopper disabled	3.1 – 3.6
0.05 Hz – 70 Hz (EEG)	Low-noise, chopper enabled	< 0.68
0.01 Hz – 5 kHz (EMG)	Low-noise, chopper enabled	< 3.9
0.1 Hz – 3 kHz (EP)	Low-noise, chopper enabled	< 3.2

### 6.3 ADC

The ADC has been measured by applying a signal to the input of the channel. Figure 13 displays the measured signal to noise (SNR) and signal to noise and distortion ratio (SNDR) versus input signal, and Figure 14 the measured output spectrum for a 70 Hz input signal with disabled chopper modulation for a data rate of 500 Hz and OSR = 256.

The measured peak SNDR for this setup is 75 dB which corresponds to an ENOB of 12.17 bits. An ENOB of more than 15.2 bits has been measured for the EEG bandwidth (0.05 Hz – 70 Hz).

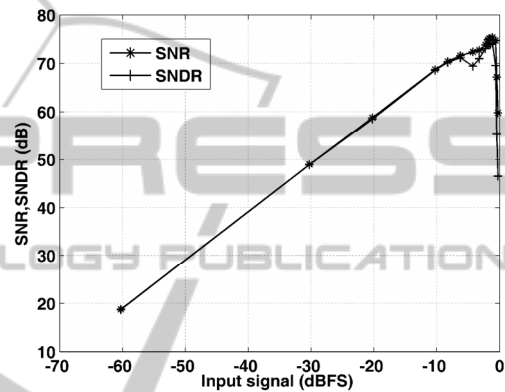


Figure 13: Measured SNR and SNDR versus input signal for a 70 Hz sine input and ECG bandwidth of 250 Hz .

### 6.4 Digital IO

The digital communication ports are tested by the setup shown in Figure 15. A C++ program running

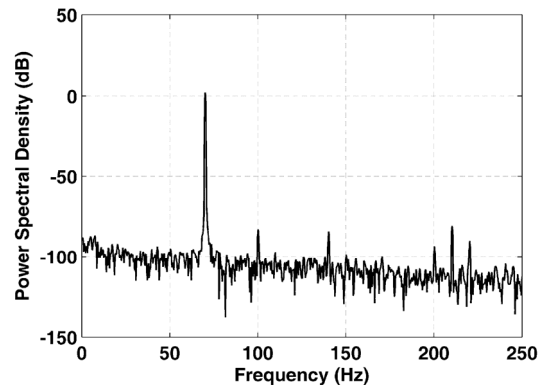


Figure 14: Measured output spectrum for 70 Hz sine input for the ECG bandwidth of 250 Hz.

on a PC communicates through the USB-interface with a Field Programmable Gate Array (FPGA) chip. The software loaded into the FPGA

implements the protocols for both serial ports of the SoC. The configuration port is tested by writing to all 100 registers with subsequent read-out of the written content and shows no missing data for a communication frequency of up to 100 kHz. The high speed serial bus was used for reading out of all channel measurements presented in this section and is operating properly for frequencies up to 55 MHz.

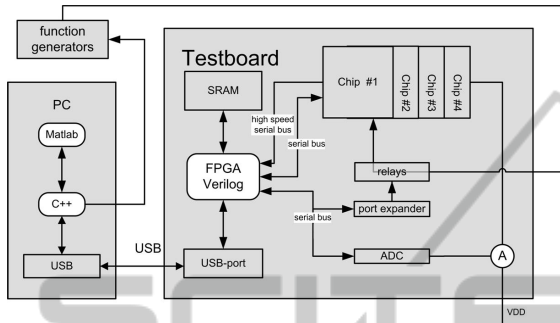


Figure 15: Test setup for the digital communication.

### 6.5 Summary

Using modern packaging technology the SoC is encapsulated in a lead free Ball Grid Array (BGA) having a size of 13 mm x 13 mm. Figure 16 shows a size comparison of the packaged SoC to a eurocent coin. The characteristics and a configuration overview of the realized biomedical SoC are summarized in Table 5 and 6, respectively.

Table 5: Main characteristics of the biomedical SoC.

Parameter	Conditions/Remarks	Value
Supply voltage		3.3 V
Current consumption	Low-power – Low-noise	8.7 mA – 63.6 mA
Total input referred noise	ECG EEG	< 1.74 $\mu$ Vpp < 0.88 $\mu$ Vpp
CMRR	@ 50/60 Hz	> 80 dB
Input common mode range	$V_{E1} = V_{Ref}$	$\pm 1$ V
Offset comp. range	High-pass & DC-suppression	$\pm 1$ V
Crosstalk	Between channels	< - 60 dB
Die area		47 mm <sup>2</sup>
Pin number		144
Package size	BGA	13 mm x 13 mm

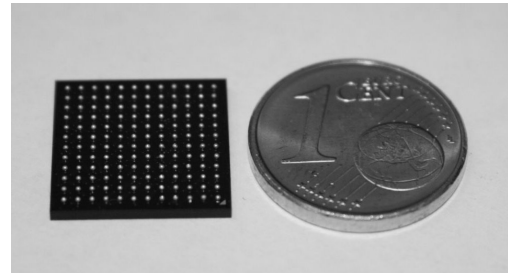


Figure 16: Photo of the SoC in a BGA package.

Table 6: SoC configuration overview.

Functional Block	Parameter	Range/ Value
Timing	Master clock divider	1 - 8
	Sample rate reduction	1 - 256
	Decimation rate	128 - 383
Analog Front-End (AFE) (adjustable per channel)	Power down	on / off
	Gain	20 / 80 / 160 / 320
	Bandwidth	3 kHz / 15 kHz
	Chopper modulation	on / off
	Bias current	$\times 1 - 16$
	CMRR calibration	64 steps
ADC (adjustable per channel)	Bias current	$\times 1 - 8$
	Data format	signed / unsigned

## 7 DISCUSSION AND CONCLUSIONS

An integrated ten channel biomedical signal acquisition system-on-chip has been presented. Each channel of the SoC includes an analog front-end that is programmable with respect to noise and power and an  $\Sigma\Delta$ -analog-to-digital converter. In addition, the system includes both a CMRR calibration and a DC-suppression circuitry. The latter extends the input-referred DC-suppression range to a remarkable value of up to  $\pm 1$  V which largely exceeds the input offset range of other integrated circuit solutions. The SoCs digital interface is realized by means of a serial configuration port and a high-speed data output port.

The implemented system-on-chip is not only suitable for multi-electrode applications, where a small system size is mandatory, but also for mobile long-term biomedical signal acquisition.

For example:

- A 100 electrode EEG system can be realized on a PCB area of less than 6 cm x 6 cm, consuming only approx. 1000 mW.

- A 9 channel ECG system would occupy only few cm<sup>2</sup> and consuming less than 50 mW. This would allow using only two standard AA batteries for an application time of more than one week (Galjan et al., 2008).

The presented SoC has been successfully employed in experimental heart rate variability tests of resting and stress test ECG recordings. At present, biomedical signal recording systems that employ the SoC are being developed and evaluated.

## ACKNOWLEDGEMENTS

The authors would wish to acknowledge Natus (formerly Schwarzer) Corporation, Munich, for their support and very fruitful discussions. The authors would also like to thank Sven Vogel for his contributions to the design and Fabian Wagner for support with the measurements.

## REFERENCES

- Martins, R., Selberherr, S., and Vaz, F. A., (1998). A CMOS IC for portable EEG acquisition systems. *IEEE Trans. Instrum. Meas.*, 47(5), 1191-1196.
- Ng, K. A., and Chan, P. K., (2005). A CMOS analog front-end IC for portable EEG/ECG monitoring. *IEEE Trans. Circuits Syst. I, Reg. Papers*, 52(11), 2335-2346.
- Yazicioglu, R. F., Merken, P., Puers, R., and Van Hoof, C., (2007). 60  $\mu$ W 60 nV/ $\sqrt{\text{Hz}}$  readout front-end for portable biopotential acquisition systems. *IEEE J. Solid-State Circuits*, 42(5), 1100-1110.
- Desel, T., Reichel, T., Rudischhauser, S., and Hauer, H., (1996). A CMOS nine channel ECG measurement IC. *2nd International Conference ASIC*.
- Fuchs, B., Vogel, S., and Schroeder, D. (2002). Universal application-specific integrated circuit for bioelectric data acquisition. *Medical Engineering and Physics* 24, 695-701.
- Martin, T., Jovanov, E., and Raskovic, D., (2000). Issues in wearable computing for medical monitoring applications: a case study of a wearable ECG monitoring device. *The Fourth International Symposium on Wearable Computers*, 43-49.
- Galjan, W., Naydenova, D., Tomasik, J. M., Schroeder, D., and Krautschneider, W. H., (2008). A portable SoC-based ECG-system for 24h x 7d operating time. In *Proceedings of IEEE Biocas 2008*, Baltimore, USA, 85-88.
- Scheer, H. J., Sander, T., Trahms, L., (2006). The influence of amplifier, interface and biological noise on signal quality in high-resolution EEG recordings. *Physiol. Meas.*, 27, 109-117.
- Bronzino, J. D., (2000). *The biomedical engineering handbook*. 2nd ed. CRC Press.
- Webster, J. G., (1998). *Medical instrumentation: application and design*. 3rd ed. Wiley & Sons, New York.
- Van Helleputte, N., Tomasik, J. M., Galjan, W., Mora-Sanchez, A., Schroeder, D., Krautschneider, W. H., and Puers, R., (2008). A flexible system-on-chip (SoC) for biomedical signal acquisition and processing. *Sens. Actuators A: Phys.*, vol. 142, Issue 1, 361-368.
- Winter, B. B., and Webster, J. G., (1983). Driven-right-leg circuit design. *IEEE Trans. Biomed. Eng.*, 30, pp. 62-66.
- Bronskowski, C. and Schroeder, D. (2006). An ultra low-noise operational amplifier with programmable noise-power trade-off. In *Proceedings 32nd ESSCIRC 2006*, Montreux, Switzerland, 368-371.
- Allen, P. E., and Holberg, D. R., (2002). *CMOS Analog Circuit Design*. Oxford University Press.
- Maxim Integrated Products, (2000). Choosing the optimum buffer / ADC combination for your application. *Application Note 1094*.
- Medeiro, F., Pérez-Verdú, B., de la Rosa, J. M., and Rodríguez-Vázquez, Á., (1997). Using CAD Tools for Shortening the Design Cycle of High-Performance  $\Sigma\Delta$ : A 16.4bit 9.6 kHz 1.71mW  $\Sigma\Delta$  in CMOS 0.7 $\mu$ m Technology. *International Journal of Circuit Theory and Applications*, 25, 319-334.
- Fuchs, B. (2004). *Integrierte Sensorschaltungen zur EKG- und EEG-Ableitung mit prädiktiver Signalverarbeitung*. PhD thesis, Institute of Nanoelectronics, Hamburg University of Technology, Shaker Verlag, Aachen.
- Dijkstra, E., Nys, O., Piguët, C., and Degrauwe, M., (1988). On the use of modulo arithmetic comb filters in sigma delta modulators. In *IEEE Proc. ICASSP88*, 2001-2004.
- Lu, A., and Roberts, G., (1994). A high-quality analog oscillator using oversampling D/A conversion techniques. *IEEE Trans. Circuits Syst. II Analog Digit. Signal Process.* 41 (7), 437-444.